NUMERICAL INVESTIGATION AND ANALYSIS ON THERMAL-HYDRAULIC CHARACTERISTICS OF DIMPLE PLATE HEAT EXCHANGER

Yubin DU [a,b], Wenjian WEI [b*], Xiaolu LI [a], Chengcheng XU [b], Guoliang XU [b]

a College of Mechanical and Electrical Engineering, China Jiliang University, Hangzhou China
b Institute of advanced heat transfer and energy application, Zhejiang University of Water Resources and Electric Power, Hangzhou China
Corresponding author Email: wenjian.wei@hotmail.com

The dimple plate heat exchanger (DPHE) has garnered attention in air-conditioning and heat pump industry due to its excellent performance. However, it is insufficient for the current research on its thermal-hydraulic performance and internal flow mechanism by varying structural parameters. In this study, numerical simulations are conducted based on flow and heat transfer cells with different dimple depths and pitches. The enhanced wall function k–ε turbulence model is employed to analyze the variation of heat transfer and frictional performance with different dimple parameters. And the internal flow mechanisms and entropy generation within the different cells are presented. The results show that the overall heat transfer factor (F) of the dimple structure approximately increases by 97.5% with the depth range of 0.7-1.5mm, while F decreases by 11.3% with the pitch of 2.8-6.0 mm. The heat transfer coefficient is more sensitive to the change in dimple depth compared to pitch. The turbulence zones within the XZ cross-section of the cell emerge and gradually shift toward the wall as the dimple depth increases or the dimple pitch decreases, which is accompanied by higher entropy generation within the cells. The new findings in present study can contribute to DPHE design optimization and promote DPHE to more practical application.

Key words: *dimple pattern, plate heat exchanger, computational fluid dynamics, entropy production*

1. Introduction

Plate heat exchangers (PHEs) are widely used in industrial sectors owing to their high efficiency, compactness, ease of maintenance, and low cost. For compact heat exchangers, the market share of PHEs exceeds 30%. In chemical processing industries, the utilization rate of PHEs is also steadily increasing, particularly in the context of efficiency improvement and carbon emissions reduction [1, 2].

Heat transfer plates exhibit a variety of geometrical features as the core components of plate heat exchangers. Among these, the chevron pattern, which has been used since the 1970s, remains the most prevalent. Extensive research has been conducted on chevron plates in existing literature. For instance, Focke *et al*.[3, 4] studied the thermal-hydraulic performance of heat transfer plates under

visualized conditions, focusing on the effects of different chevron angles. Muley *et al.*[5, 6] investigated the variation in the heat transfer and pressure drop with the chevron angle and corrugation aspect ratio. They observed that both the Nusselt number and friction factor increased with the chevron angle, corrugation aspect ratio, and core flow velocity in a heat transfer plate. Hessaim *et al.*[7] compared the performance of heat transfer plates with chevron angles of 45^o and 60^o and, revealed the flow mechanisms within the plates at different angles. Wang *et al.* [8]employed a multi-objective optimization approach to conduct computing fluid dynamics (CFD) simulations on double-chevron plate-shell heat exchangers and identified the optimal structural parameters for thermal performance.

In addition, heat-transfer plates featuring uniformly distributed circular dimples have attracted significant attention. Song *et al.* [9] proposed a hexagonal dimple plate heat exchanger, using a three-inlet, three-outlet flow configuration. The results revealed that this novel plate heat exchanger significantly outperformed a conventional 60^o chevron plate heat exchanger. In recent years, the research team of the authors haves been investigating a novel dimple plate heat exchanger called micro-plate heat exchanger (MPHE) featuring a large number of dimple-like cavities. Wei *et al.* [10] conducted experimental comparisons between a new heat exchanger and conventional exchangers. The results showed that the MPHE exhibited a superior heat transfer performance and a lower pressure drop. Additionally, Zhang *et al.* [11] performed numerical simulations on the MPHE within a Reynolds number range of $800 < Re < 4000$, selecting five simulated units and employing the SST k-ω turbulence model. Under these conditions, the predicted Nusselt number had a relative error of ±32% compared with the experimental results, while the friction coefficient was within ±23%. Li *et al.* [12] conducted a visualization analysis of MPHE channels using high-speed cameras to explain the bubble generation patterns inside the channels by varying inlet and outlet conditions. Mocnik *et al.*[13-15] compared the experimental results with CFD simulations of the MPHE. They found that the k-ε turbulence model with enhanced wall functions was in good agreement with experiments at low Reynolds numbers ($70 < Re < 469$), particularly when $Re > 100$, showing a closer match with the internal flow patterns observed in the experiments. In the range of $1000 < Re < 4000$, both the k-ε turbulence model and Reynolds Stress Model demonstrated fair agreement with their experimental data. Wei *et al.*[16] conducted an experimental study on the flow distribution of refrigerant R410A in chevron-pattern plate and two different dimpled plate structures, the results showed that the refrigerant exhibited better lateral flow in the fish-scale dimpled structure compared to the traditional dimpled plate. Tao *et al.*[17] demonstrates that dimpled plate heat exchangers with flexible flow section areas improve heat pump performance in cold environments by enhancing heat transfer and mitigating mass flux imbalance, achieving a 62% improvement in the overall heat transfer coefficient compared to chevron plate heat exchangers.

Some researchers have employed the second law of thermodynamics to investigate the thermal-hydraulic performance of plate heat exchangers, which accounts for the irreversibility of evaluating the energy losses during the heat transfer process. Bejan and Kestin[18] was the first to propose the use of the entropy generation principle to analyze heat transfer performance in fluid flow based on the second law of thermodynamics. Johannessen *et al.*[19] demonstrated that when the local entropy generation in each part of the system is constant, the entropy generation due to heat exchange within the heat exchanger is minimized, and they proposed a counterflow heat exchanger as the

optimal configuration for heat transfer. Guo *et al.*[20] utilized entropy minimization methods to optimize the performance and analyze the transient processes of heat exchangers.

Recently developed dimpled structures offer more design flexibility and involve a greater number of structural parameters, such as depth, dimple size, dimple pitch, dimple shape, and dimple arrangement. However, in our research group's previous studies, performance tests[10], numerical model validation[11], and flow distribution analysis[16] within the plates were conducted for a specific structure of the dimpled plate heat exchanger. In addition, recent papers published on dimple plate structures have not addressed the impact of varying dimple depth and pitch on the thermal-hydraulic performance[13-15]. Zhang[21] found that dimple depth and dimple pitch are the most sensitive parameters affecting thermal performance, although no quantitative relationships were provided. Therefore, this study focuses on these two parameters and investigated their influence on the thermal performance of dimpled structures.

In order to investigate the thermal-hydraulic performance variations of dimpled plate heat exchangers with different structural parameters, this study utilizes numerical simulations to examine the effects of varying dimple depths and pitches on heat exchanger performance, as well as the sensitivity of these parameters on the overall efficiency of the dimpled structure. In addition, entropy generation theory is employed to quantify the energy losses within the flow cell and analyze the irreversibility associated with different structural configurations. The results of this study provide valuable insights for the design of these two parameters in practical engineering applications of dimpled plate heat exchangers. Furthermore, the conclusions can be integrated with the analysis of irreversibility to enable the optimization of structural parameters for enhanced performance.

2. Methodology

2.1. Problem description

Figure 1 shows a schematic of the dimpled structure, the subject of this study is consistent with the objects investigated in the research group’s previously published papers[10, 11], the key structural parameters of this configuration are shown in the Fig. 1, while the structural parameters selected for this study are listed in Tab. 1.

The selection of these structural parameters is based on the practical applications of dimpled plate heat exchangers, under the dimple depths 0.7-1.5mm and the dimple pitches 2.8-6.0mm. The chosen dimple depth and pitch cover the structural parameters commonly used in actual applications. The thermal-hydraulic performance corresponding to these parameters can provide valuable insights for the practical design of dimpled plate heat exchangers, helping to understand how the thermal-hydraulic performance changes with variations in structural parameters. Additionally, this study reveals the sensitivity of the thermal-hydraulic performance to these two structural parameters.

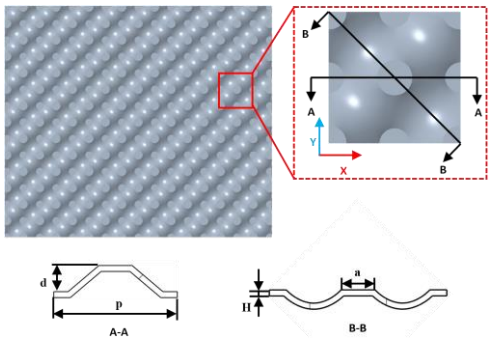

Fig. 1. Schematic diagram of the dimple plate structure

Table 1. Structural parameters for CFD simulations

Parameter	Value
Thickness, *H*[mm]	0.25
Depth, *d*[mm]	0.7-1.5 with intervals of 0.2 @fixed pitch of 5.2mm
Pitch, *p*[mm]	2.8-6 with intervals of 0.8 @fixed depth of 1.1mm
Dimple diameter, *a*[mm]	A quarter of the pitch

2.2. Governing equations

The geometric model is simplified by considering time-consuming and computational resources and the focus of the analysis. Non-critical components, such as rounded corners, are neglected. In the actual production process of dimpled plate heat exchangers, very small rounded transition structures may appear at the edges of the dimple features to facilitate demolding of the plate stamping dies. However, this part is ignored in the CFD calculations. Including these rounded structures in the dimple features would significantly increase the complexity of the model, making mesh generation more difficult and requiring greater computational resources. Ignoring the rounded edges does not alter the fundamental dimple features, and since the main objective of this study is to investigate the effects of dimple depth and pitch on thermal-hydraulic performance, the effects of these microstructures on the actual fluid flow are relatively negligible compared to other structural parameters, and the influence of these rounded edges was excluded from consideration. The distribution of dimple structures on the plates is periodic, and a portion of the dimple features is extracted for numerical computation to reduce the number of elements and computational complexity. Despite these simplifications, the geometric model adequately represented the primary heat transfer pathways and fluid flow characteristics of the actual structure.

The solid parts of the model were assumed to be homogeneous materials and the surface roughness was neglected. Additionally, the contact thermal resistance between the solids was ignored because of the small contact area and thickness between the plates. In this study, water is used as the working fluid, and some assumptions are applied: single-phase, incompressible, steady flow, and stable turbulent flow in three-dimensional space. The fundamental relationships for calculating incompressible fluids are based on the mass, momentum, and energy conservation equations, which are expressed as Eqs. (1)-(3), respectively:

$$\frac{\partial \rho}{\partial t} + \nabla \cdot (\rho \vec{v}) = s_m \tag{1}$$

$$\frac{\partial}{\partial t}(\rho\vec{v}) + \nabla\cdot(\rho\vec{v}\vec{v}) = -\nabla p + \nabla\cdot(\tau) + \rho\vec{g} + \vec{F} \tag{2}$$

$$\frac{\partial}{\partial t}(\rho E) + \nabla\cdot(\vec{v}(\rho E + p)) = \nabla\cdot(k_{eff}\nabla T - \sum_j h_j J_j + (\vec{\tau}_{eff}\cdot\vec{v})) + S_h \tag{3}$$

2.3. Numerical method

A modeling approach for dimple-patterned plates was first developed, followed by the selection of numerical computation targets. Subsequently, the mesh generation and independence verification were conducted. The thermal performance differences were explored by analyzing the flow field trajectories to reveal the potential causes. Finally, the principle of entropy generation was applied to quantify the irreversible losses incurred during the heat exchange process, with the aim of further analyzing the heat transfer enhancement mechanisms and potential pathways associated with the point-wave structure. The detailed computational procedure is illustrated in Fig. 2.

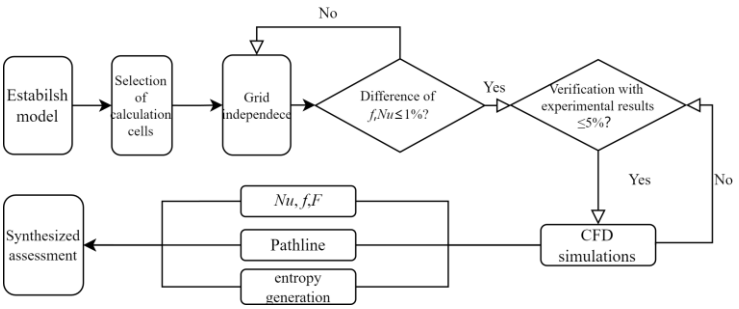

Fig. 2. Flow chart of calculation and analysis

The study employed a comprehensive assessment index for quantitative analysis to facilitate the evaluation of the performance in different plate structures, and the definition of this index is provided in Eq. 4.

$$F = Nu / f^{1/3} \tag{4}$$

where Nu is the Nusselt number defined as $Nu = h_w D / \lambda_f$, and h_w represents the water heat transfer coefficient over the dimple plate and is calculated by $q/(T_w - T_f)$, where q is the heat flux imposed over the heat transfer surface, and T_w and T_f are the plate wall and fluid temperatures, respectively. λ_f is the fluid thermal conductivity, and D is the hydraulic diameter of the characteristic region[14].

The friction factor was calculated using the Eq. (5). Where ΔP is the pressure drop across the channel, ρ denotes the fluid density, L is the channel length of the characteristic region, and v_m is the mean viscosity of the fluid in the characteristic region.

$$f = \frac{\Delta P D}{2\rho L v_m^2} \tag{5}$$

The entropy generation rate is used to characterize the rate of entropy generation at various points within the channel[22], denoted as $\dot{S}'''_{gen}$, which represents the addition of the irreversible losses at the heat transfer surface, $\dot{S}'''_{gen,\Delta T}$, and the flow resistance losses in the fluid, $\dot{S}'''_{gen,\Delta P}$, as expressed by:

$$\dot{S}'''_{gen} = \dot{S}'''_{gen,\Delta T} + \dot{S}'''_{gen,\Delta P} \tag{6}$$

$$\dot{S}'''_{\mathrm{gen},\Delta T} = \frac{\lambda_f}{T^2}\left[\left(\frac{\partial T}{\partial x}\right)^2 + \left(\frac{\partial T}{\partial y}\right)^2 + \left(\frac{\partial T}{\partial z}\right)^2\right] \tag{7}$$

$$\dot{S}'''_{gen,\Delta P} = \frac{\mu}{T}\left\{2\left[\left(\frac{\partial u}{\partial x}\right)^2 + \left(\frac{\partial v}{\partial y}\right)^2 + \left(\frac{\partial w}{\partial z}\right)^2\right] + \left(\frac{\partial u}{\partial x} + \frac{\partial v}{\partial y}\right)^2 + \left(\frac{\partial u}{\partial x} + \frac{\partial w}{\partial z}\right)^2 + \left(\frac{\partial v}{\partial y} + \frac{\partial w}{\partial z}\right)^2\right\} \tag{8}$$

Figure 3(a) presents the structural model used for the numerical calculations. The model adopted a symmetrical three-channel heat transfer mode with four stacked plates. According to a the study by Zhang *et al*. [23], fluid flow within the plate stabilizes after passing through 3-5 cells. Therefore, a 3×6 cell configuration was selected in this study. Figure 3(b) presents the channel model used for numerical calculations. The red areas represent the plates, while the other regions denote the fluid domains. The central fluid region was of interest in this study, and the top and bottom plates were not included in the simulation. The fluid inlets, labeled inlets 1, 2, 3 were oriented in opposite directions to simulate the symmetrical counterflow conditions observed in the experiment. Additionally, a 30mm stabilization region was set at both the inlet and outlet to eliminate the entrance effect and ensure a fully developed flow in the characteristic region.

A second-order upwind scheme was employed for discretization based on the finite volume method in a numerical simulation. Convergence was assumed when the outlet temperature, pressure drop across cells, and heat flux over the surface stabilized with residuals less than 10^{-6}. According to the report of Močnik *et al*. [13], the realizable *k-ε* turbulence model with enhanced wall functions performed better for dimple structures compared to other models. Therefore, a realizable *k-ε* model with enhanced wall functions was applied in this study.

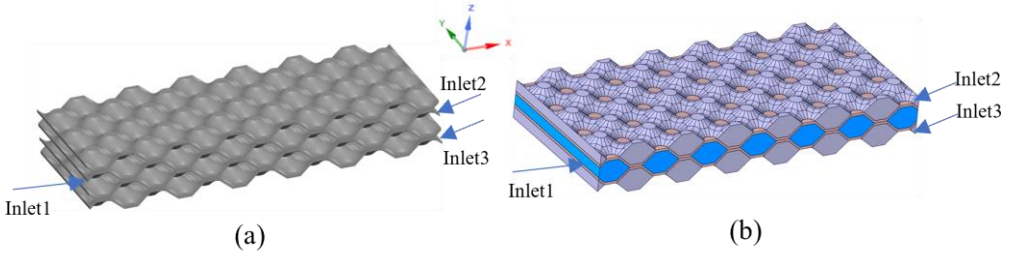

Fig. 3. Schematic diagram of the dimple plate assembly used for numerical simulation

The inlet was set to a mass flux boundary condition to ensure a consistent average fluid velocity in the characteristic region across models with different structural parameters. The mass fluxes at inlets 2 and 3 were kept constant, with a mass flux of 58.3 kg/m^2·s, and the inlet temperature was maintained at 50 °C. The heat-transfer characteristics were compared under different inlet conditions by adjusting the mass flux at inlet 1, with the fluid velocity in the characteristic region ranging from approximately 0.05 to 0.2 m/s. The detailed boundary conditions for each case are presented in Tab. 2.

The boundary conditions in Tab. 2 were selected based on practical operational conditions and study's objectives. The range of inlet mass flux values (58.3-174.8 kg/m²·s) was chosen to cover typical operating conditions of plate heat exchangers used in industrial and commercial applications, particularly to air-conditioning and heat pump system, with the Reynolds number 100-5000. And the inlet temperature represents a realistic condition for hot water used in heat transfer applications, ensuring relevance to practical systems. This temperature was kept constant to isolate the effects of

mass flux on heat transfer and flow characteristics. The plate material's thermal conductivity was set to 16.8 W/m·K, representing stainless steel, which is commonly used in plate heat exchangers due to its excellent mechanical and thermal properties.

Table 2. Boundary conditions

Parameters	Value				
	case1	case2	case3	case4	case5
Fluid	Water				
Inlet mass flux, [$kgm^{-2}s^{-1}$]	58.3	87.4	116.5	145.7	174.8
Temperature, [^oC]	65				
Plate thermal conductivity, [$Wm^{-1}K^{-1}$]	16.8				

2.4. Grid independence and CFD model validation

A polyhedral mesh is used for grid generation rather than traditional tetrahedral meshes because of its lower memory consumption, lower computation time cost, and fewer elements with the same accuracy[24]. The results of the grid-independence verification are presented in Tab. 3.

In Tab. 3, when the grid size reached 4.8 million elements, the discrepancies in the pressure drop and *Nu* compared to the 5.9 million element case were less than 0.5%. Therefore, it can be concluded that the mesh is no longer a factor influencing the results, and this mesh generation strategy will be applied to models with other structural parameters.

A numerical comparison was performed based on the experimental conditions and parameters from Zhang *et al*. [11], using the above numerical calculation method. Figure 4 shows the results of the calculation and the experimental data. Specific detailed information that was not mentioned by Zhang *et al*. [11] about the experimental equipment and operating conditions can be found in Wei *et al*.[25], which provides detailed parameters of the tested objects and the description of experimental setup. The single-phase testing platform is consistent with that used by Zhang et al. It reveals that deviations between the numerical data and experimental data from Zhang *et al*. are within 3%, which indicates that the numerical method is credible and reliable for further calculations in the present study.

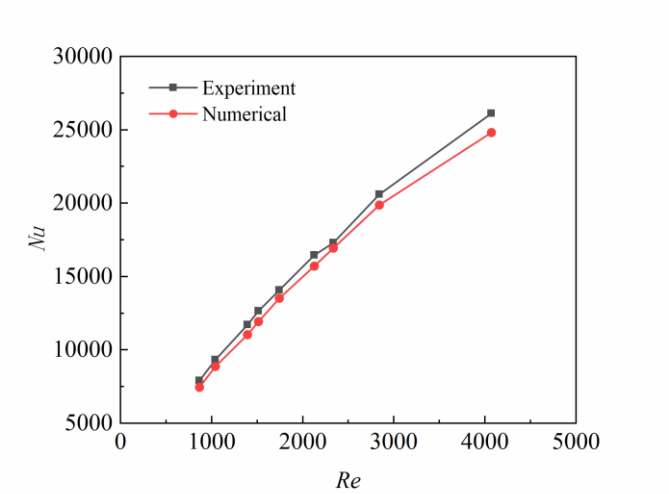

Fig. 4. Comparisons between numerical results and experimental results

Table 3. Grid independence study at G = 58.3kg/m^{2}s for p = 5.2mm and a = 1.1mm

No. of cells [10^6]	Difference in pressure drop	Difference in *Nu*
1.7	2.95%	4.84%
2.5	1.48%	2.39%
3.8	0.93%	1.72%
4.8	0.13%	0.14%
5.9	-	-

3. Results and discussion

3.1. The effect of dimpled-plate parameters on heat transfer

Figure 5(a) illustrates the variation in *Nu* with different dimple depths and pitches. *Nu* increases as the dimple depth increases under identical inlet conditions, with an approximate increase of 122.3% with the depth of 0.7-1.5mm. Conversely, Fig. 5(a) demonstrates that *Nu* decreases with increasing dimple pitch under the same inlet conditions. Specifically, *Nu* decreases by approximately 28.4% with the pitch range of 2.8-6.0mm.

3.2. The effect of dimpled-plate parameters on pressure loss

The variation in *f* with depth and pitch is shown in Fig. 5(b). As shown in Fig. 5(b) the friction factor *f* monotonically increases with dimple depth. This indicates that *f* shows a steady upward trend as the depth increases under the same inlet conditions, and increases by approximately 42.8% with the depth of 0.7-1.5mm. Figure 5(b) reveals a trend similar to that of *Nu*, where *f* decreases by approximately 47.6% with the pitch variation 2.8-6.0mm under the same inlet conditions.

3.3. The effect of dimple-plate parameters on overall performance

Figure 5(c) illustrates the variation in the overall performance factor *F* with depth. It can be observed that *F* also increases with depth. The average increase in *F* was approximately 97.5% with the depth 0.7-1.5mm. Figure 5(c) shows that, *F* exhibits a decreasing trend when the pitch changes, Although the overall decrease is not significant, it decreases by a minimum of 8.2% and a maximum of 16.3% under different mass fluxes with the pitch 2.8-6.0mm.

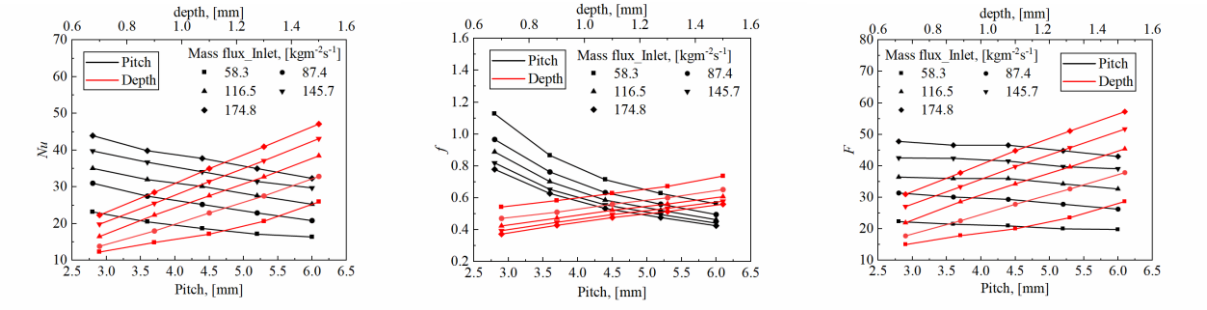

(a) (b) (c)

Fig. 5. Variations of (a)*Nu*, (b)*f*, (c)*F* with depth and pitch for different mass flux

As mentioned above, *Nu*, *f*, and *F* increase with an depth and decrease with the increase in pitch under the structural parameters considered in this study. However, *F* was not highly sensitive to pitch changes. This suggests that while reducing the dimple pitch can enhance the heat transfer to some extent, the resulting pressure loss is significant and cannot be ignored. Therefore, pitch is not the key factor affecting the overall heat transfer and flow resistance compared to depth in practical engineering applications. In industrial applications, minimizing pressure drop while maximizing heat transfer efficiency is crucial for improving energy performance and reducing operational costs. Although smaller pitch values might increase heat transfer, they also significantly increase the pressure loss, leading to higher pumping costs, which could negate the benefits of enhanced heat transfer. As a result, the optimal design of PHEs should prioritize the balance between heat transfer enhancement (by increasing depth) and the associated pressure loss. This study suggests that for commercial plate heat exchangers, wave depth is a more influential design parameter than pitch in determining the heat exchanger's overall performance, especially in terms of minimizing energy consumption and operational costs in real-world applications.

4. Further discussion

Figure 6 illustrates the flow streamlines within the XZ and XY cross-sections of a single flow cell. Flow streamlines were selected for the case with an inlet mass flux of 116.5 kg/m^{2}s due of the similarity in the variation patterns under different inlet conditions. Figures 6(a) and (b) show the streamlines in the XZ plane at different depths and pitches, respectively. In Fig. 6(a), it can be observed that vortices formed by secondary flow gradually emerge as the depth increases from 0.7 to 1.5mm. The vortex region moved closer to the wall with increasing depth. During the heat transfer within the plate, owing to the presence of the boundary layer, more intense heat transfer occurs near the wall. Therefore, vortices near the wall enhance the heat transfer, which explains why larger dimple depths result in both improved heat transfer capacity and higher pressure loss.

In contrast, as shown in Fig. 6(b), a vortex region exists in structures with smaller pitches. The vortex region moves away from the wall as the pitch increases, which is the opposite trend to that observed when the depth is changed. When the pitch increases further, the vortex phenomenon disappears, indicating that structures with smaller dimple pitches exhibit superior thermal-hydraulic performance. Additionally, changes in vortex behavior within the cross-section were more pronounced at different depths compared to variations in pitch. This explains why the overall heat transfer coefficient is more sensitive to depth than to pitch.

Figures 6 (c) and (d) show the streamlines within the XY cross-section. Its impact on the thermal-hydraulic performance of the dimple structure is minimal, and changes in the flow are relatively small because this region is farther from the core heat transfer zone near the wall. The flow streamlines in this region display an opposite pattern to that in the XZ cross-section: at larger dimple depths, the vortex phenomenon is less pronounced, whereas at larger dimple pitches, a more noticeable vortex behavior occurs. Thus, the flow streamlines in the XY cross-section can also assist researchers in analyzing the thermal-hydraulic performance of dimple structures.

In practical heat transfer processes, the heat transfer enhancement is closely related to the variation in the structure of the transfer surface, which is accompanied by irreversible energy losses and entropy generation. These energy losses can be used for an in-depth analysis of the influences of the surface or channel structure on the heat transfer characteristics. Therefore, this study examined entropy production within flow cells to further explore the relationship between entropy generation heat transfer capacity of dimple structures.

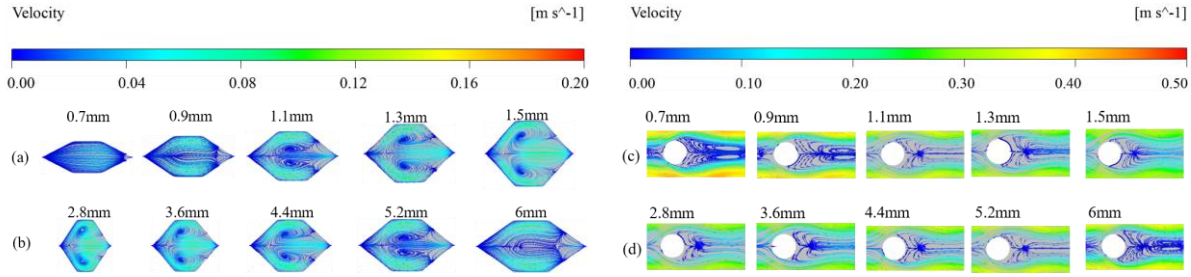

Fig.6. Streamline of single flow cell；(a)XZ cross-section with depth, (b) XZ cross-section with pitch, (c) XY cross-section with depth, (d) XY cross-section with pitch

Figures 7 (a) and (b) depict the entropy generation resulting in heat transfer and flow in the X-Z plane, respectively. And Figs.7 (c) and (d) show entropy generation of those two categories in the X-Y plane. From a numerical perspective, irreversible losses caused by heat transfer are dominant during the flow and heat transfer processes. Additionally, in the X-Z plane, the regions of entropy generation are mostly concentrated near the wall, which is understandable given the more pronounced boundary layer effects in this region. Figure 8 shows the heat transfer and flow entropy generation for different pitches. As shown in Fig. 7, that hat entropy generation increases monotonically with depth in both the X-Z and X-Y planes. However, the entropy generation gradually decreases the increasing dimple pitch in the XZ and XY cross-sections, as shown in Fig. 8.

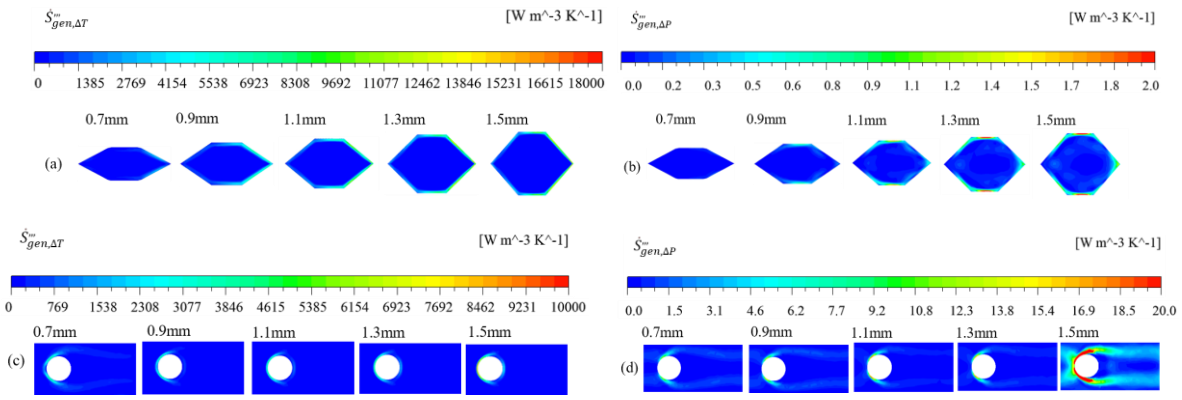

Fig. 7. Entropy generation contour with different depth in single flow cell. (a) Heat transfer entropy generation in XZ cross-section, (b) Flow entropy generation in XZ cross-section, (c)Heat transfer entropy generation in XY cross-section, (d) Flow entropy generation in XY cross-section

Combined with the patterns of heat transfer capacity and friction factor described in Section 3, the entropy generation trends in Figs. 7 and 8 align well with these findings. As the dimple depth increases, entropy generation increases, whereas as the dimple pitch increases, entropy generation decreases. This suggests a close relationship between entropy generation within the flow cell and the thermal-hydraulic performance of the dimple structure. This analysis highlights an important design trade-off: while a deeper dimple can enhance heat transfer, it also leads to higher energy dissipation, which could increase the operational cost due to higher pumping power required to overcome pressure losses. Conversely, increasing the dimple pitch could reduce energy dissipation, but the corresponding reduction in heat transfer efficiency may not be desirable in commercial plate heat exchangers, where maximizing heat exchange while minimizing energy consumption is crucial.

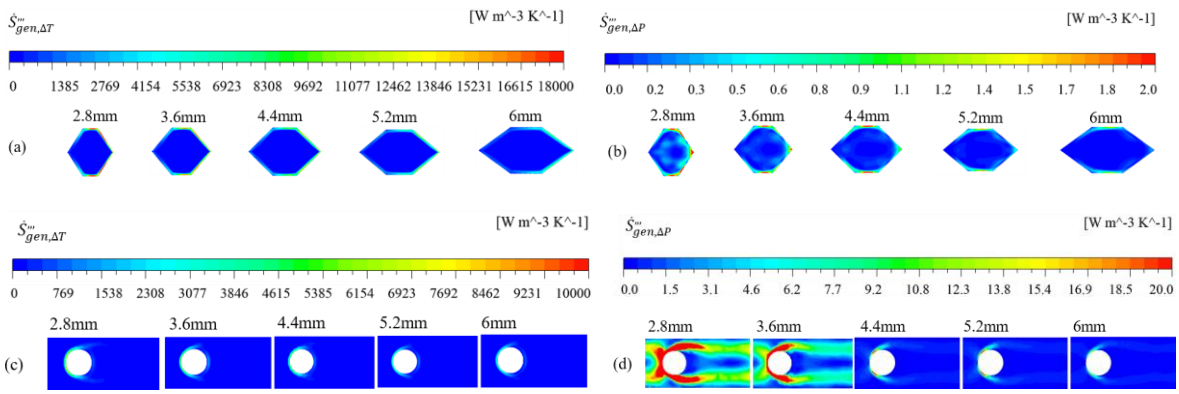

Fig. 8. Entropy generation contour with different pitch in single flow cell；(a)Heat transfer entropy generation in XZ cross-section, (b) Flow entropy generation in XZ cross-section, (c) Heat transfer entropy generation in XY cross-section, (d) Flow entropy generation in XY cross-section

5. Conclusions and prospectives

In this study, numerical simulations were conducted on dimpled plate heat exchangers. The accuracy of the numerical model was validated using experimental data. In a total of 50 cases, with dimple depths 0.7-1.5mm and dimple pitches 2.8-6.0mm, and five different inlet flow rates for each structural parameter, the thermal-hydraulic performance trends of the dimpled structure and the sensitivity of these two parameters on overall performance were investigated. Additionally, energy losses within the flow cell were analyzed to study the variations in irreversible losses under different structural parameters. The main conclusions of this study are as follows:

- Heat transfer, pressure drop and comprehensive efficiency increases with dimple depths and decreases with the increasing of dimple pitch, i.e. *Nu*, *f*, and *F* increase by 122.3%, 42.8%, and 97.5%, respectively with the depths 0.7-1.5mm by fixing the inlet mass flux and dimple pitch of 4.0 mm, while decrease by 28.4%, 47.6%, and 11.3%, respectively under the dimple pitch 2.8-6.0mm by fixing the dimple depth to 1.2mm.
- The heat transfer of dimpled plate heat exchangers can be enhanced by generating the symmetric vortex flows within the plate channels, particularly perpendicular to flow direction (XZ plane).
- Both dimple depth and pitch are associated with greater irreversibility losses. Dimple depth seem more significantly impact on overall performance and is considered as a more critical parameter for optimizing heat exchanger performance in practical applications.

Further research will be conducted to optimize the key dimpled geometric parameters using methods such as topology optimization or genetic algorithms, with the aim of achieving the optimal performance of dimpled plate heat exchangers and performing practical validation. This is crucial for the development of the next generation of dimpled plate heat exchangers.

Declaration of Competing Interest

The authors declare that there are no competing interests.

Nomenclature

a – Dimple diameter, [m]
A – Area, [m^2]
D – Hydraulic diameter, [m]
d – Corrugation depth, [m]
f – Friction coefficient, [-]
F – Performance factor, [-]
G – Mass flux, [$kgm^{-2}s^{-1}$]
h – Heat transfer coefficient, [$Wm^{-2}K^{-1}$]
H – Thickness, [m]
L –Length, [m]
Nu – Nusselt number, [-]
p – Pitch, [m]
q – Heat flux, [Wm^{-2}]
Re – Reynolds number, [-]
$\dot{S}'''$ – Entropy, [$Wm^{-3}K^{-1}$]
T – Temperature, [K]
v – Velocity, [ms^{-1}]

Greek symbols

ΔP – Pressure drop, [Pa]
ρ – Density, [kgm^{-3}]
λ – Thermal conductivity, [$Wm^{-1}K^{-1}$]

Subscripts

f – fluid
gen – generation
m – mean
s – surround
w – wall

References

[1] Zhang, J., *et al.*, A review of heat transfer enhancement techniques in plate heat exchangers, *Renewable and Sustainable Energy Reviews, 101* (2019), pp. 305-328
[2] Zohuri, B., *Compact heat exchangers*, Springer, Cham, Switzerland, 2017
[3] Focke, W., *et al.*, The effect of the corrugation inclination angle on the thermohydraulic performance of plate heat exchangers, *International Journal of Heat Mass Transfer, 28* (1985), 8, pp. 1469-1479
[4] Focke, W., Turbulent convective transfer in plate heat exchangers, *International Communications in Heat Mass Transfer, 10* (1983), 3, pp. 201-210
[5] Muley, A., *et al.*, Enhanced heat transfer characteristics of viscous liquid flows in a chevron plate heat exchanger, *Journal of Heat and Mass Transfer, 121* (1999), 4, pp. 1011-1017
[6] Muley, A., Manglik, R.M., Enhanced heat transfer characteristics of single-phase flows in a plate heat exchanger with mixed chevron plates, *Journal of Enhanced Heat Transfer, 4* (1997), 3, pp. 187-201
[7] Hessami, M.A., An experimental investigation of the performance of cross-corrugated plate heat exchangers, *Journal of Enhanced Heat Transfer, 10* (2003), 4, pp. 379-394
[8] Wang, K., *et al.*, CFD simulation and optimization study on the shell side performances of a plate and shell heat exchanger with double herringbone plates, *Thermal Science and Engineering Progress, 43* (2023), p. 101931
[9] Song, J., *et al.*, Experimental study and analysis of a novel multi-media plate heat exchanger, *Science China Technological Sciences, 55* (2012), pp. 2157-2162
[10] Wei, W., Li, H., Experimental analysis of fluid flow heat transfer and pressure loss characteristics in dimpled plate heat exchangers, *Chinese Journal of Refrigeration technology, 32* (2012), 04, pp. 36-41(in Chinese language)
[11] Zhang, R., *et al.*, Numercial investigation and analysis of fluid flow and heat transfer of single-phase in dimpled plate heat exchanger, *Chinese Journal of Refrigeration technology, 34* (2014), 05, pp. 6-12(in Chinese language)
[12] Li, X., *et al.*, Visualization of bubble flow in the channel of a dimple-type embossing plate heat exchanger under different fluid inlet/outlet ports, *International Journal of Heat Mass Transfer, 145* (2019), p. 118750
[13] Močnik, U., *et al.*, Numerical and experimental analysis of fluid flow and flow visualization at low Reynolds numbers in a dimple pattern plate heat exchanger, *Energy, 288* (2024), p. 129812
[14] Močnik, U., Muhič, S., Experimental and numerical analysis of heat transfer in a dimple pattern heat exchanger channel, *Applied Thermal Engineering, 230* (2023), p. 120865
[15] Močnik, U., *et al.*, Numerical Analysis with Experimental Validation of Single-Phase Fluid Flow in a Dimple Pattern Heat Exchanger Channel, *Journal of Mechanical Engineering/Strojniški Vestnik, 66* (2020), 9, pp. 544-553
[16] Wei, W., *et al.*, Flow Characteristics and Optimization of Two-phase Flow Distribution over Plate Surface of Brazed-Plate Heat Exchanger, *Chinese Journal of Refrigenration, 45* (2024), 1, pp. 46-54(in Chinese language)
[17] Tao, X., *et al.*, Flow boiling in dimpled plate heat exchangers with different geometric parameters: Analysis of asymmetric channels, *Applied Thermal Engineering, 257* (2024), p. 124265
[18] Bejan, A., Kestin, J., *Entropy generation through heat and fluid flow*. John Wiley & Sons. New York, USA, 1983.
[19] Johannessen, E., *et al.*, Minimizing the entropy production in heat exchange, *International Journal of Heat Mass Transfer, 45* (2002), 13, pp. 2649-2654
[20] Guo, J., *et al.*, Optimization design of shell-and-tube heat exchanger by entropy generation minimization and genetic algorithm, *Applied Thermal Engineering, 29* (2009), 14-15, pp. 2954-2960
[21] Zhang, Z., Optimization of the transition surface in asymmetric dimpled plate evaporators, Master thesis, Zhejiang university, Hangzhou, China, 2024.

[22] Bejan, A., *et al.*, *Thermal design and optimization*. John Wiley & Sons. New Jersey, USA, 1995.
[23] Zhang, L.Z., Numerical study of periodically fully developed flow and heat transfer in cross-corrugated triangular channels in transitional flow regime, *Numerical Heat Transfer, Part A: Applications*, *48* (2005), 4, pp. 387-405
[24] Peric, M., Ferguson, S., The advantage of polyhedral meshes, *Dynamics*, *24* (2005), 45, p. 504
[25] Wei, W.J., *et al.* Experimental investigations on performance of evaporator and condenser of R410A inside a novel brazed plate heat exchanger, *Proceedings*, Proceedings of the 24th IIR International Congress of Refrigeration, Yokohama, Japan, 2015

Submitted: 24.11.2024.

Revised: 18.01.2025.
Accepted: 24.01.2025.